Proceedings of the 4th International Conference on Biological Engineering and Medical Science
DOI: 10.54254/2753-8818/40/20241209

Delivery of differentiation therapy into solid tumor cancer stem-like cells to prevent metastasis and recurrence

Zezhi Zhou

BASIS International School Guangzhou, Huangpu District, Guangzhou, Guangdong, China

zhouzez@outlook.com

Abstract. The concept of differentiation therapy offers an attracting explanation for plenty of clinical observations, such as relapse and metastasis. Its hallmark success has been in the treatment of acute promyelocytic leukaemia, a condition that is now highly curable through the combination of retinoic acid (RA) and arsenic. Recently, the finding of cancer stem-like cells (CSCs) triggers more attentions due to it's unique high tumourigenicity and chemoresistance., which reside in hypoxic tumor regions, and are characterized by high tumourigenicity and chemoresistance. Considerable efforts have been made to develop promising anti-CSC strategies, including blocking surface biomarkers and inhibiting self-renewal signaling pathways. In this study, we engineered a liposomal delivery strategy that enables the codelivery of RA and arsenate, aiming to differentiate and potentiate CSCs. The core of the liposome is formed through coordination polymerization between arsenate and Calcium, while the membraneincorporates RA and helper lipids. We evaluated their cytotoxicity against cultured CSCs and their potential to differentiate CSCs into less malignant phenotypes.

Keywords: differentiation therapy, cancer stem cells, liposome

1. Introduction

The theory of cancer stem-like cells (CSCs) is inspired from the observation that only a small fraction of tumor cells is capable of tumor initiation and growth. This subpopulation of cancer cells is defined as the CSCs, which possess distinct phenotypic characteristics from bulk tumor cells, such as self-renewal and epithelial-mesenchymal transition [1]. These properties are referred to as stemness. The maintenance of stemness is achieved through multiple interrelated pathways, including phosphatidylinositol 3-kinase (PI3K)/Akt/mammalian target of rapamycin (mTOR), NOTCH, hedgehog, and Wnt/β-catenin [2]. The CSC theory provides convincing explanations for plenty of clinical observations. For example, the relapse of tumors after traditional chemotherapy and/or radiotherapy is considered to be mediated by CSCs, as CSCs are refractory to most chemotherapeutics or ionizing radiation. The approaches by which CSCs develop resistance include upregulated pro-survival pathways, inhibited apoptosis, dormancy cycling, and efflux transporters [3-4]. In addition, the existence of CSCs also explains metastasis of tumor, where CSCs migrate out of the primary tissue and form distal nodules owing to their tumor initiation capacity [4].

Recently, differentiation therapy has been reported as a promising strategy with a specific target for those CSCs [5]. The concept of differentiation therapy is derived from the fact that hormones and

© 2024 The Authors. This is an open access article distributed under the terms of the Creative Commons Attribution License 4.0 (https://creativecommons.org/licenses/by/4.0/).

DOI: 10.54254/2753-8818/40/20241209

cytokines can promote differentiation ex vivo, thereby irreversibly changing the phenotype of cancer cells. Its hallmark success has been demonstrated in the treatment of acute promyelocytic leukemia, a type of CSC-enriched cancer. It is now highly curable with the combination of retinoic acid (RA) and arsenate. Recently, differentiation therapy has gained more attention due to the discovery of CSCs in solid tumors, which reside in hypoxic tumor niches and are characterized by high tumourigenicity and chemoresistance [6]. The existence of CSCs has been evidenced as the chief culprit of progression, recurrence, and metastasis in multiple malignancies. The presence of CSCs is significantly higher in poorly differentiated tumors compared to well-differentiated counterparts, which results in higher-grade malignancy and poorer prognosis [5, 7]. Considerable efforts have been made to develop promising anti-CSC strategies, including blocking the surface biomarkers and inhibiting the self-renewal signaling pathways. However, these strategies are usually limited due to the lack of targetable CSC markers and the turnover plasticity of CSC [8-10].

Currently, RA and arsenate still remain the most powerful agents against CSCs. However, their pharmacokinetics are unfavorably distinct for synergy. In addition, the free molecules in the circulation system are extremely subjective to urinal clearance and enzymatic degradation. In order to optimize the delivery of RA and arsenate into CSCs, we engineered a liposomal delivery strategy that enables the co-delivery of RA and arsenate, aiming to differentiate and potentiate CSCs. The core is formed through coordination polymerization between arsenate and calcium and the membrane is formed with RA and helper lipids. We hypothesize that simultaneous loading of these two synergistic agents will synchronize their release kinetics and improve their synergistic index. Moreover, we will evaluate its capability to reduce stemness, with the goal of avoiding potential relapse and metastasis.

2. Materials and methods

2.1. Coordination liposome synthesis

The aqueous solution of sodium arsenate (2 mg, 10 mg/mL) dissolved in deionized water and DOPA (4 mg, 200 mg/mL in $CHCl_3$) was added dropwise to 5 mL of 0.3 M Triton X-100/1.5 M 1-hexanol in cyclohexane and stirred vigorously for 15 min. Then, an aqueous solution of $Ca(NO_3)_2$ (20 mg, 100 mg/mL) was added to a 5 mL of 0.3 M Triton X-100/1.5 M 1-hexanol in cyclohexane and stirred vigorously for 5 min. The $Ca(NO_3)_2$-containing microemulsion was added dropwise to the Arsenate-containing microemulsion and stirred vigorously for 30 min at room temperature. After the addition of 10 mL ethanol, bare particles were obtained by centrifugation at 14000 rpm. The bare particles were dried under nitrogen and decomposed with metal-grade nitric acid to measure the As loading with ICP-MS. The resulting pellet was washed once with THF/ethanol and finally redispersed in THF. RA/As liposome was prepared by adding a THF solution (80 μL) of As bare particles, cholesterol, DOPC, DSPE-PEG2k (1:0.4:0.8:1.5 by mass) and RA (equivalent to As by number of mols) to 500 μL of 30% (v/v) ethanol/water at room temp. The mixture was stirred at 1700 rpm for 1 min. THF and ethanol were completely evaporated under nitrogen.

2.2. Cell culture

Human carcinoma cells MDA-MB-468 were purchased from American Type Culture Collection (Rockville, MD, USA) and cultured as suggested methods in Dulbecco's Modified Eagle's Medium (DMEM), supplemented with 10% fetal bovine serum, 100 U/mL penicillin G sodium, and 100 g/mL streptomycin sulfate.

For tumorsphere culture of MDA-MB-468 cell lines, MDA-MB-468 cells were allocated into the ultralow attachment flask in 5 mL of serum-free medium which contains DMEM/Ham's F12 (1:1), epidermal growth factor (EGF, 20 ng/ml), basic fibroblast growth factor (bFGF, 10 ng/ml) both from PeproTech (Rocky Hill, NJ, USA), 0.5% B27 supplement (Thermal Fisher, United States) and 1% P/S. Cells were allowed to from spheroid for 7 days.

DOI: 10.54254/2753-8818/40/20241209

2.3. In vitro cytotoxicity

MDA-MB-231 stem cells were seeded in 96-well plates at a density of 2,000 cells/well. Cells were then treated with different concentrations of As liposomes, RA liposomes, or As/RA liposomes for 72 hours. Cell viability was quantified by 3-(4,5-dimethylthiazol-2-yl)-5-(3-carboxymethoxyphenyl)-2-(4-sulfophenyl)-2H-tetrazolium assay (Promega, Madison, MI) according to manufacturer's instructions. The cell viability was evaluated with plate reader using absorbance at 490 nm.

2.4. Spheroid assay

MDA-MB-468 stem cells were allocated into the ultralow attachment 96-well plate in 200 μL of serum-free medium which contains DMEM/Ham's F12 (1:1), epidermal growth factor (EGF, 20 ng/ml), basic fibroblast growth factor (bFGF, 10 ng/ml) both from PeproTech (Rocky Hill, NJ, USA), 0.5% B27 supplement (Thermal Fisher, United States) and 1% P/S. Experimental groups were treated with the same medium supplemented with 0.1 μM of As liposomes, RA liposomes, or As/RA liposomes. Cells were allowed to form spheroid for 7 days. The number of tumor spheroids was counted under an optical microscope.

2.5. Flow cytometry

MDA-MB-468 stem cells were seeded into the ultralow attachment 6-well plate in 2 mL of serum-free medium which contains DMEM/Ham's F12 (1:1), epidermal growth factor (EGF, 20 ng/ml), basic fibroblast growth factor (bFGF; 10 ng/ml) both from PeproTech (Rocky Hill, NJ, USA), 0.5% B27 supplement (Thermal Fisher, United States) and 1% P/S. Experimental groups were treated with the same medium supplemented with 1 μM of As liposomes , RA liposomes, or As/RA liposomes for 24 hours. The spheroids were digested with collagenase, and filter with a membrane filter (pore size, 40 μm) to obtain single-cell suspension. To quantify the expression of Yamanaka transcription factors, the cells were permeabilized with 0.03% v:v Triton-X/PBS and blocked with 5% Bovine Serum Albumin in PBS for 1 hour. The blocked cells were then stained with Sox2-AF647 antibodies according to the manufacturer's protocol. The stained cells were analyzed with flow cytometry (LSR II, BD).

3. Results

3.1. Synthesis and characterization of coordination liposomes

The synthesis of coordination liposomes involves two steps: the reverse emulsion and self-assembly, as shown in **Fig. 1**. The synthesized coordination liposomes contain a metallic core formulated through coordination polymerization between arsenate and Calcium. Then the core formed with reversed emulsion was coated with helper lipids via self-assembly. As a result, the final liposomes contain biocompatible metals, and a bi-layered lipid membrane, as shown in **Fig. 1**. To visualize their formulated morphology, we imaged the nanoparticles with transmission electron microscopy (TEM). We found that the liposomes were monodispersed with spherical structures for AS/RA, as well as corresponding control liposomes which contains either arsenate (AS) or retinoic acid (RA) (**Fig. 2A-C**). Due to the low electron density of the lipid bilayer, only the electron-dense core is visible under TEM. The TEM images of RA/AS also confirmed the successful formation of coordination liposomes.

To quantitatively evaluate the sizes of formulated liposomes, we measured their hydrodynamic diameter using Dynamic Light Scattering (DLS). Their size distributions were shown in **Fig. 2D**. We found that the particles all monodispersed distribution with excellent polydisperse index (PDI), which is shown in **Table 1**. The PDI reflects molecular mass distribution and dispersion was measured to be 0.189 for RA, 0.199 for AS, and 0.196 for RA/AS. Technically, an acceptable PDI should be below 0.7 for drug delivery application, whereas our liposomes have PDIs below 0.2, which indicates the uniformed property. RA, AS, and RA/AS have average hydrodynamic radius of 68.7 nm, 67.7 nm, and 58.9 nm. The drug loading of arsenate was determined via inductively coupled plasma mass spectrometry, and we designed the RA:AS molecular ratio to be equal to 1:1.

DOI: 10.54254/2753-8818/40/20241209

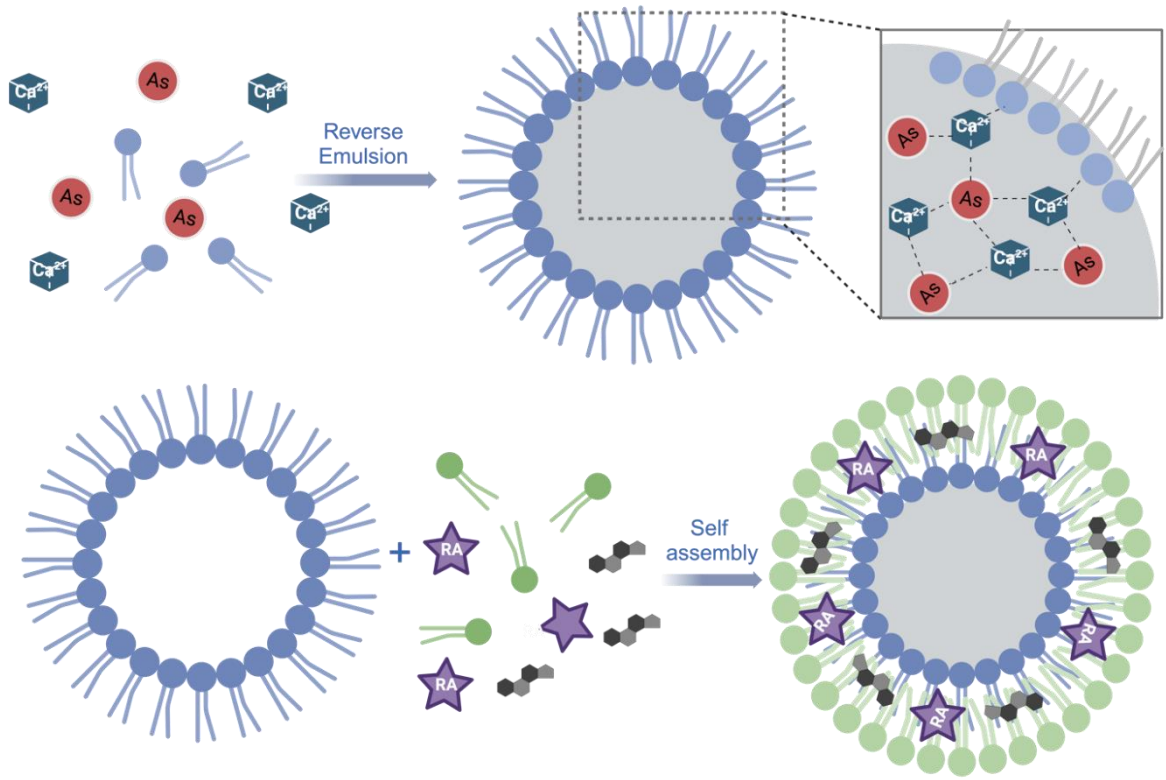

Figure 1. Synthesis of coordination liposomes from two steps: reverse emulsion and self-assembly.

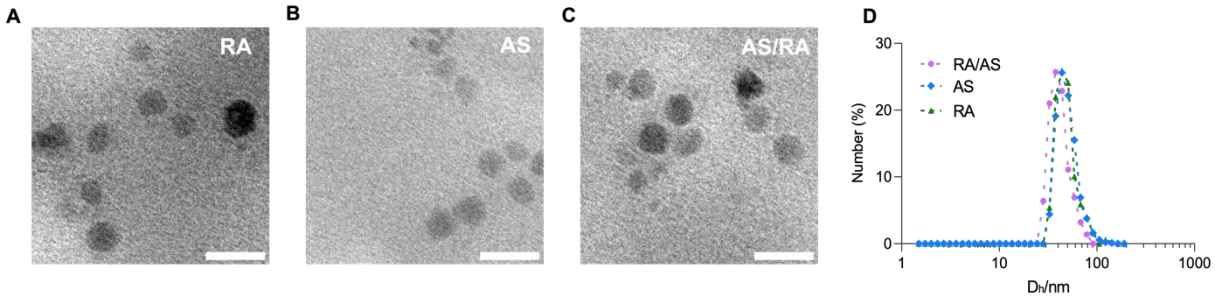

Figure 2. Characterization of synthesized coordination liposomes. (A) TEM image of RA. (B) TEM image of AS (C) TEM image of RA/AS (D) Hydrodynamic distribution of coordination liposomes. Scale bar, 50nm.

Table 1. The hydrodynamic radius of coordination liposomes

Liposomes	Hydrodynamic Radius/nm	PDI
RA	68.7	0.188
AS	67.7	0.199
RA/AS	58.9	0.196

3.2. Synergistic cytotoxicity of RA/AS coordination liposomes

After successfully synthesized the coordination liposomes, we would like to know whether retinoic acid and arsenate persist synergistic effect against cancer cells, as delivery system tends to reshape the pharmacokinetic and pharmacodynamic properties of drugs. We adopted a human triple-negative breast cancer cell, MDA-MB-468, to test their synergistic cytotoxicity *in vitro*. We first measured their drug

DOI: 10.54254/2753-8818/40/20241209

concentration-cell viability curve and regressed with sigmoidal function, as show in **Fig. 3A**. The IC50 of RA, AS, and RA/AS was determined to be 3.3μM, 1.86μM, and 0.39μM, respectively. In order to determine whether retinoic acid and arsenate are in synergy, we quantified their combination index following the equation below:

$$Combination\ Index\ (CI) = \frac{IC50\ of\ RA\ (combinatorial)}{IC50\ of\ RA\ (alone)} + \frac{IC50\ of\ AS\ (combinatorial)}{IC50\ of\ AS\ (alone)}$$

When the CI is below 1, we consider the activity of RA and AS in our liposome to be synergistic. When the CI exceeds 1, we consider the activity to be antagonistic. We found in all different effective levels, the CI is consistently below 1 in **Fig.3B**. Thus, we concluded that RA/AS synergized retinoic acid and arsenate, even though delivery system can alter their pharmacokinetics and pharmacodynamics.

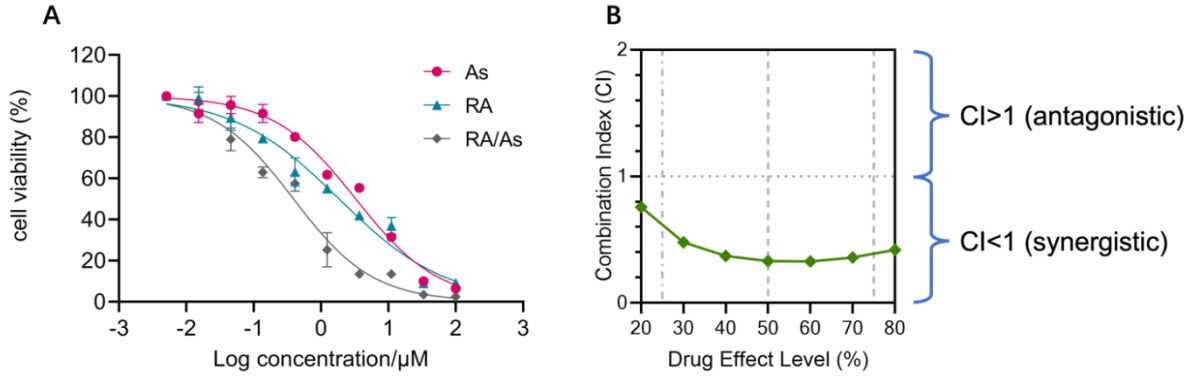

Figure 3. Synergistic cytotoxicity against MDA-MB-231 cells. (A) Synergistic cytotoxicity of RA/AS revealed by cytotoxicity assay. (B) Combination index calculated.

3.3. Reduced cancer stemness features after RA/AS treatment

After confirming the synergistic effect of retinoic acid and arsenate achieved in our system, we would like to further explore their application in differentiation therapy. We enriched the cancer stem-like cells (CSCs) by adopting serum-free method of cell culture, which avoid the differentiation of CSCs by depleting growth factors from fetal bovine serum. Thus, the CSCs could maintain their undifferentiated phenotype in the culture. The bulk cancer cells of MDA-MB-468 grown in serum-rich medium were monolayered, while the enriched MDA-MB-468 CSCs were grown in spheroid, as shown in **Fig. 4A and 4B**.

In order to determine whether RA/AS is able to differentiate CSCs to reduce stemness features, we first adopted spheroid assay to check the regeneration and self-renewal ability of CSCs after treatment. We found that, by supplementing RA/AS liposomes, the MDA-MB-468 CSCs lost their ability to regenerate, which indicates their phenotypic change by genetic reprogramming (**Fig. 4C**). Unsurprisingly, the RA and AS alone also showed ability to reduced stem features, but lower than RA/AS.

Then, we would like to quantitatively measure to what extent the stemness features have been decreased. Hence, we used flowcytometry to quantify the expression level of a 'Yamanaka' factor, Sox2, which is a crucial transcription factor to maintain CSC phenotypes. To perform single-cell analysis of MDA-MB-468 CSCs, we first selected the live cells, which should have highest granularity, from side scattering. We then clustered the singular cell in forward scattering. Finally, we measured that the expression level of Sox2, which was reduced by RA/AS as shown in **Fig. 4D**. This implicated that our liposomes are capable of reprogramming and eradicate CSCs, offering the opportunity of inhibiting cancer metastasis and relapse induced by refractory CSCs.

DOI: 10.54254/2753-8818/40/20241209

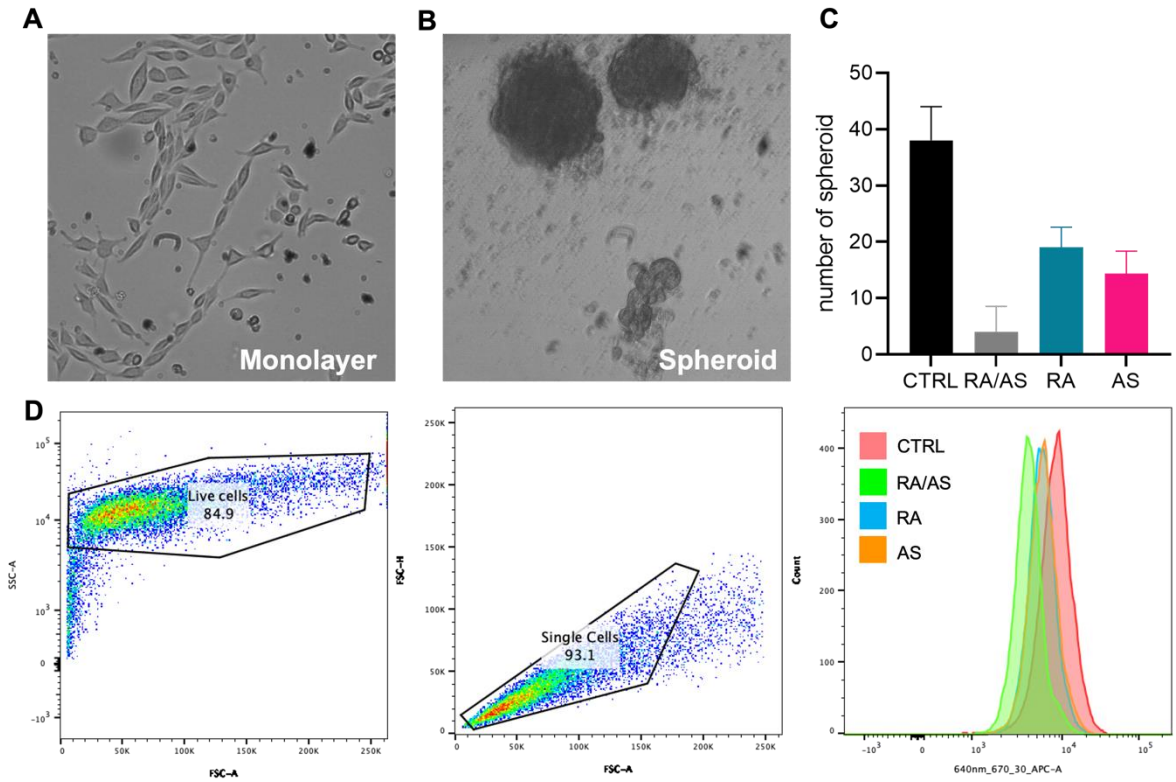

Figure 4. The reduced stemness features of MDA-MB-468 stem cells. (A) Bulk MDA-MB-468 cancer cells grown in monolayer. (B) MDA-MB-468 cancer stem cells grown in tumor spheroid. (C) Spheroid assay for stemness evaluation. (D) Reduced expression of Sox2 stemness marker measured by flow cytometry.

4. Conclusion and discussion

Cancer is having a global impact on people's lives. Existing conventional treatment strategy such as chemotherapy and radiotherapy are effective, but the evolutionary nature of tumor can exhaust these on-hand tools. CSCs are one of the driving forces for tumor to evolve and develop resistance to state-of-art therapies. In contrast, differentiation therapy reshapes the characteristics of CSCs by genetic reprogramming, which provides an attracting solution to eradicate refractory CSCs. Here, by simultaneously encapsulating arsenate and retinoid acid and delivering them to the CSCs by a well-synthesized liposome, we demonstrated synergistic cytotoxicity and stemness reduction in a human breast cancer CSCs. The advantages of adopting a lipid-coated solid nanoparticle to deliver arsenate is multifactorial. First, the synthesis and the loading of the arsenate into the particle can be performed in mild conditions. This suggests that incorporating additional functions, such as targeting modules, into our system is achievable. Second, our RA/AS nanoparticle has a coordination core which fixes the arsenate to minimize undesired drug release under physiological pH.

Admittedly, there are still questions that need further investigation in our research. First, the loading ratio of retinoic acid and arsenate has not been optimized to maximize their synergistic effect. Second, it is crucial to success the pharmacokinetic and pharmacodynamic profiles to evaluate the performance in real circulation systems. Third, even though we have confirmed the RA/AS can decrease CSC stem features *in vitro*, the conclusion remains to be validated *in vivo* with experimental animals. Last but not least, the eradication of CSCs can significantly prevent the systemic metastasis and post-surgery recurrence. This capability of our synthesized liposomes was yet confirmed. Future study might be interesting to evaluate this using designated animal models. Although there are some limitations, this

project still achieves the purpose of demonstrating the effectiveness of differentiation therapy via delivery liposome, which provide a new perspective for cancer therapy.

References

[1] Phi, L. T. H.; Sari, I. N.; Yang, Y.-G.; Lee, S.-H.; Jun, N.; Kim, K. S.; Lee, Y. K.; Kwon, H. Y., Cancer Stem Cells (CSCs) in Drug Resistance and their Therapeutic Implications in Cancer Treatment. *Stem Cells Int* 2018, *2018*, 5416923-5416923.

[2] Batlle, E.; Clevers, H., Cancer stem cells revisited. *Nature Medicine* 2017, *23* (10), 1124-1134.

[3] Schulz, A.; Meyer, F.; Dubrovska, A.; Borgmann, K., Cancer Stem Cells and Radioresistance: DNA Repair and Beyond. *Cancers (Basel)* 2019, *11* (6), 862.

[4] Shiozawa, Y.; Nie, B.; Pienta, K. J.; Morgan, T. M.; Taichman, R. S., Cancer stem cells and their role in metastasis. *Pharmacol Ther* 2013, *138* (2), 285-293.

[5] Ingangi, V.; Minopoli, M.; Ragone, C.; Motti, M. L.; Carriero, M. V., Role of Microenvironment on the Fate of Disseminating Cancer Stem Cells. *Frontiers in Oncology* 2019, *9* (82).

[6] Kathagen, A.; Schulte, A.; Balcke, G.; Phillips, H. S.; Martens, T.; Matschke, J.; Günther, H. S.; Soriano, R.; Modrusan, Z.; Sandmann, T.; Kuhl, C.; Tissier, A.; Holz, M.; Krawinkel, L. A.; Glatzel, M.; Westphal, M.; Lamszus, K., Hypoxia and oxygenation induce a metabolic switch between pentose phosphate pathway and glycolysis in glioma stem-like cells. *Acta Neuropathologica* 2013, *126* (5), 763-780.

[7] Meacham, C. E.; Morrison, S. J., Tumour heterogeneity and cancer cell plasticity. *Nature* 2013, *501* (7467), 328-337.

[8] Chae, Y. C.; Kim, J. H., Cancer stem cell metabolism: target for cancer therapy. *BMB Rep* 2018, *51* (7), 319-326.

[9] Tan, S.; Li, D.; Zhu, X., Cancer immunotherapy: Pros, cons and beyond. *Biomed Pharmacother* 2020, *124*, 109821.

[10] Lytle, N. K.; Barber, A. G.; Reya, T., Stem cell fate in cancer growth, progression and therapy resistance. *Nature Reviews Cancer* 2018, *18* (11), 669-680.